Acta din Croat 2002; 41 (Suppl): 41-51 Review

MAGNETIC RESONANCE IMAGING OF LIVER LESIONS

Miljenko Marotti, Ratimira Klarić-Čustović, Ivan Krolo, Nenad Babić

Department of Diagnostic and Interventional Radiology, Sestre milosrdnice University Hospital, Zagreb, Croatia

SUMMARY – With the introduction of breath-hold techniques, magnetic resonance (MR) imaging has become an excellent diagnostic tool for the detection and characterization of benign and malignant liver lesions. Dynamic, gadolinium postcontrast studies as well tissue-specific contrast media highly improve the characterization of liver lesions. Multisection breath-hold techniques enable imaging of the entire region of interest in a single suspended respiration. MR-cholangiopancreatography allows for simultaneous analysis of biliary tree and pancreatic duct. The ability of various MR pulse sequences to display differences between normal and pathologic tissues is the basis of detection and characterization of focal and diffuse liver changes.

Cyst

Ultrasound (US), computed tomography (CT) and magnetic resonance imaging (MRI) have similar possibilities in detection and evaluation of cystic lesions. On MRI, simple cysts are shown as round or oval, sharply defined homogeneous lesions with very low signal intensity on T1 weighted images and homogeneous very high signal intensity on T2 weighted images[1]. On postcontrast scans, they resemble void signal intensity (Fig. 1). Hemorrhagic cysts show an increase of signal intensity according to time of bleeding[2]. Septa and daughter cysts in case of echinoccocus are well visualized as linear structures within the cyst (Figs. 2a, b). TRUFI and HASTE breath-hold sequences show cysts as high signal intensity lesions (Fig. 2c). Occasionally abscesses have similar morphology as cysts (Fig. 3).

Correspondence to: *Prof. Miljenko Marotti, M.D., Ph.D.,* Sestre milosrdnice University Hospital Department of Diagnostic and Interventional Radiology, Vinogradska 29, HR-10000 Zagreb, Croatia

Hemangioma

Differentiation of hemangiomas from other focal liver lesions is of great importance, as they occur in 1% to 20% of the population[3,4]. The majority of hemangiomas are asymptomatic measuring from few millimeters to 20 centimeters, and require no treatment. Sometimes (15%) they produce the symptoms of nausea, abdominal pain and vomiting due to rupture, hemorrhage or extrinsic compression of adjacent structures. Hemangiomas have a female/male ratio of 5:1, and are multiple in 50% of patients. The usual US description of hemangioma is that of a well defined, rounded, echogenic homogeneous lesion, usually less than 2 centimeters in size. Sometimes, hemangiomas on US show a hypoechoic inhomogeneous pattern, making impossible differentiation from other necrotic liver tumors[5,6].

Hemangiomas are hypodense on native CT scans, whereas on dynamic postcontrast scans they exhibit marked edge enhancement.

On MRI, hemangiomas appear as low-signal intensity lesions on T1 weighted images (Fig. 4a, 4b), whereas on T2 weighted images they display a high-intensity appearance[7,8] (Fig. 4c) . The areas of low-signal intensity correspond with fibrous tissue. MRI is very sensitive in

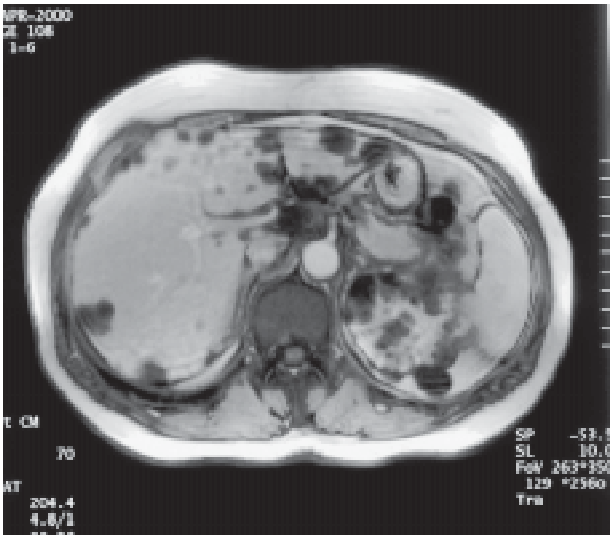

Fig. 1. Polycystic disease. Postcontrast breath-hold in phase sequence with multiple liver and kidney cysts without enhancement after administration of GD-DTPA.

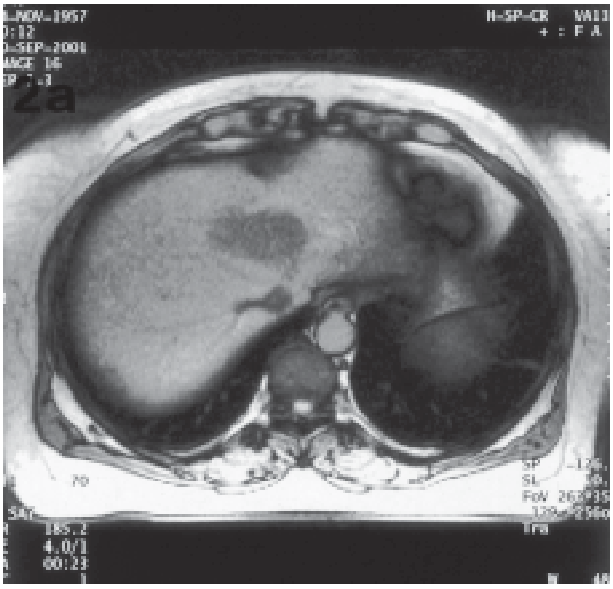

Fig. 2a Echinococcus cyst. Breath-hold out of phase sequence showing a low to medium signal intensity cyst.

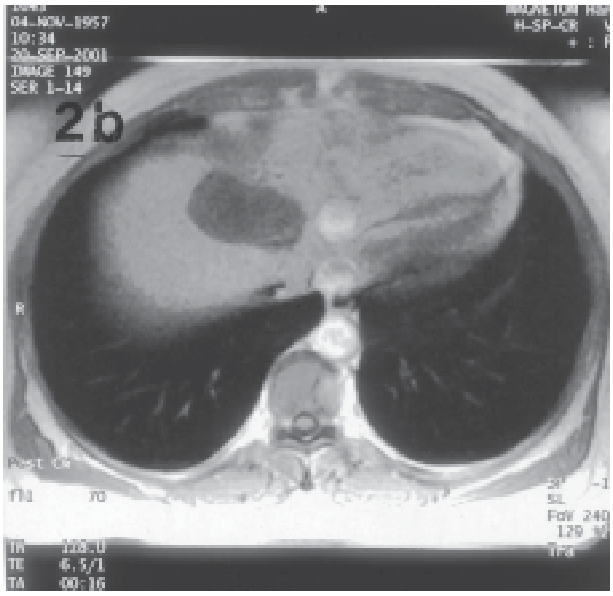

Fig. 2b. Postcontrast breath-hold out of phase sequence showing discrete linera septa within unenhanced echinococcus cyst.

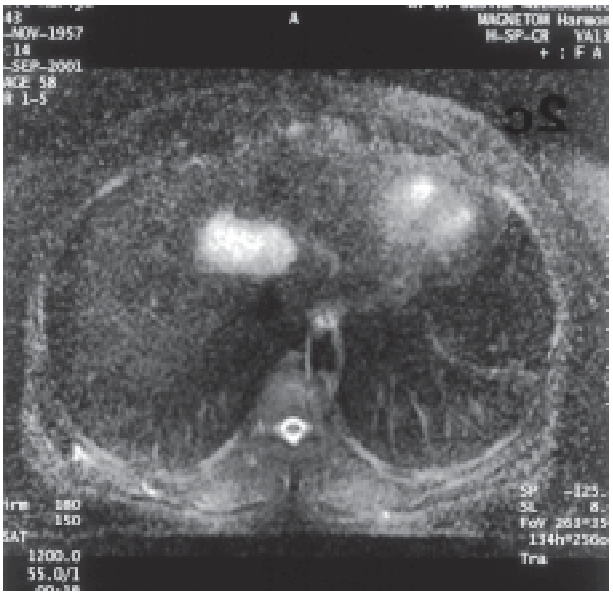

Fig. 2c. On HASTE sequence, the cyst is of a high signal intensity.

detection and differentiation of hemangiomas from other focal liver lesions, whereas on T2 weighted images with very long TR they hold high-intensity appearance, opposite to other solid and cystic lesions. Breath-hold techniques enable dynamic postcontrast studies which demonstrate hemangiomas as edge nodular enhancing lesions in the arterial phase with central hypointensity, due to large peripheral feeding vessels[9,10] (Fig. 4d). Small hemangiomas (less than 2 cm) demonstrate uniform enhancement and on delayed scans they become isointense with liver parenchyma. Some large hemangiomas have a central stellate area similar to the central scar of focal nodular hyperplasia (FNH), and exhibit nodular enhancement progressing centripetally. The scar in hemangioma has low signal intensity on T2 weighted images due to fibrous tissue[11]. The central scar of FNH consists of rich

Fig. 3 Breath-hold out of phase oblique postcontrast sequence. Postcholecystectomy abscess in the gallbladder fossa.

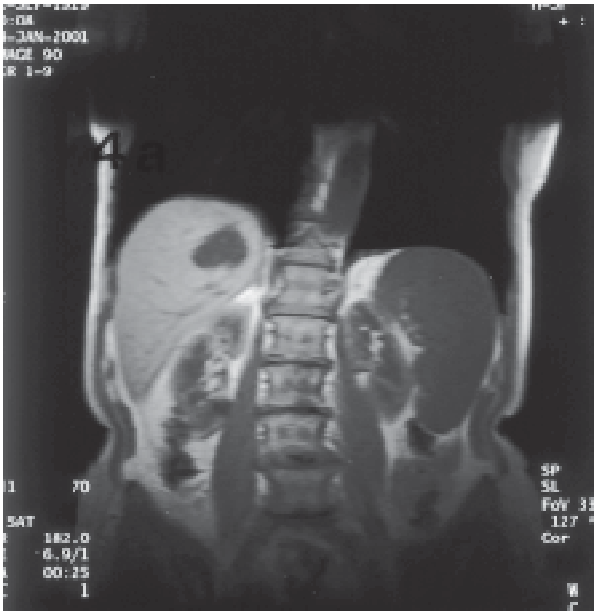

Fig. 4a Breath-hold in phase coronal sequence showing a hemangioma of low signal intensity.

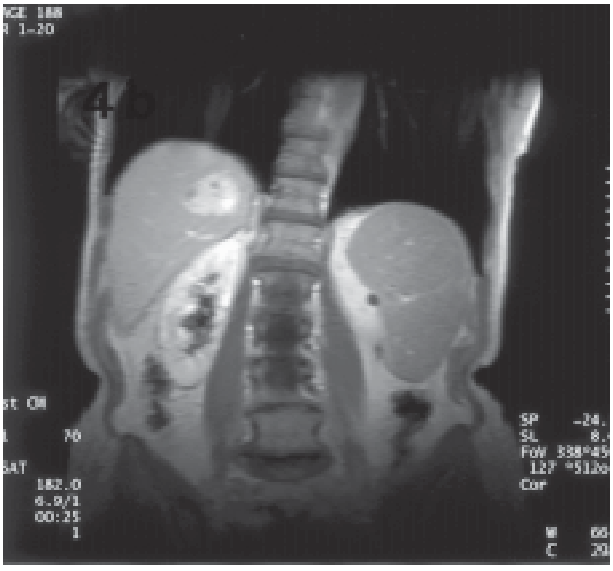

Fig. 4b. Postcontrast breath-hold in phase coronal sequence showing homogeneous diffuse enhancement of the lesion.

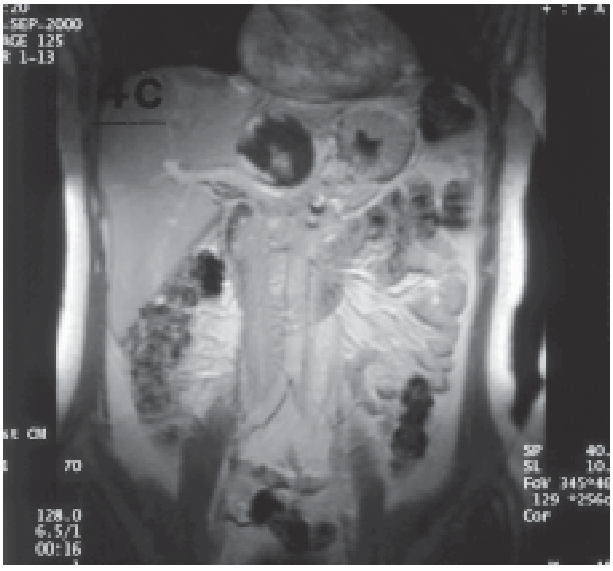

Fig. 4c. Postcontrast breath-hold in phase coronal sequence showing edge enhancement of the lesion.

vascular fibrous tissue and exhibits high signal intensity on T2 weighted images[12-14]. Metastases from endocrine tumors may have extremely high signal intensity and can be misdiagnosed as hemangiomas. Confirmation of hemangioma is possible after administration of SPIO particles with strong increase of signal intensity on postcontrast T1 weighted images[15].

Focal Nodular Hyperplasia and Hepatocellular Adenoma

According to one report, CT is less sensitive in detection of FNH than US[7]. Hepatic adenomas cannot be differentiated on the US basis from FNH. MRI has been reported to be able to detect the central scar not detect-

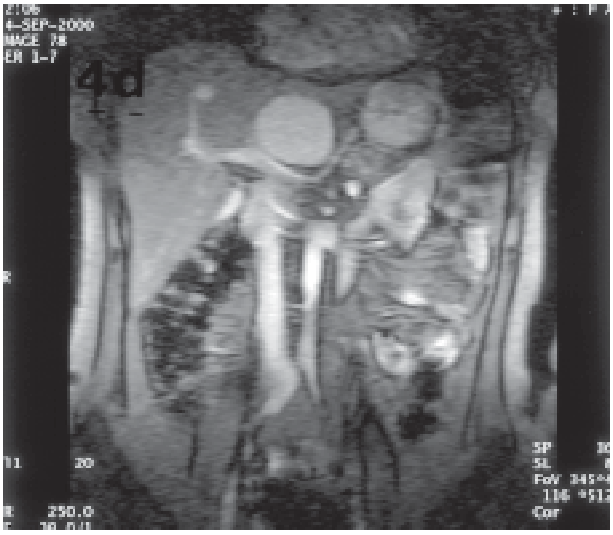

Fig. 4d Breath-hold T2 weighted image showing homogeneous high signal intensity of hemangioma.

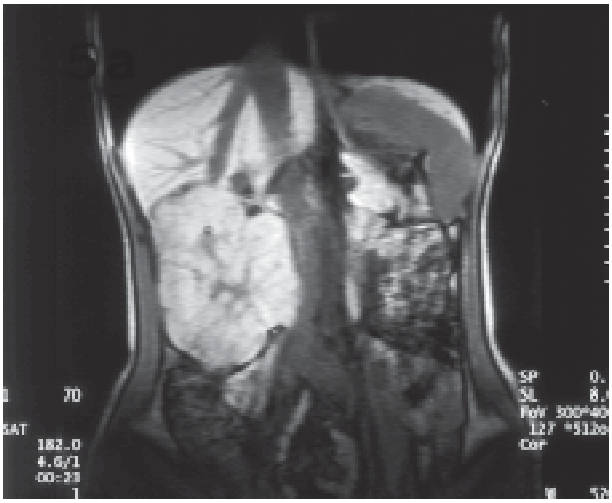

Fig. 5a Breath-hold out of phase coronal image of focal nodular hyperplasia. The lesion is mostly of extrahepatic location with a central scar.

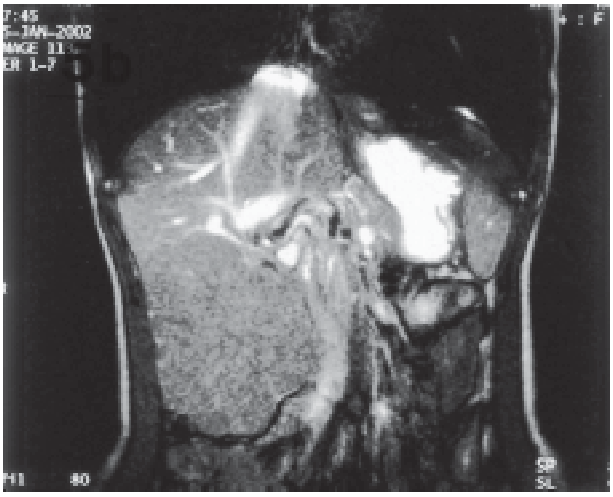

Fig. 5b. Breath-hold T2 weighted image. Focal nodular hyperplasia is isointense with liver parenchyma.

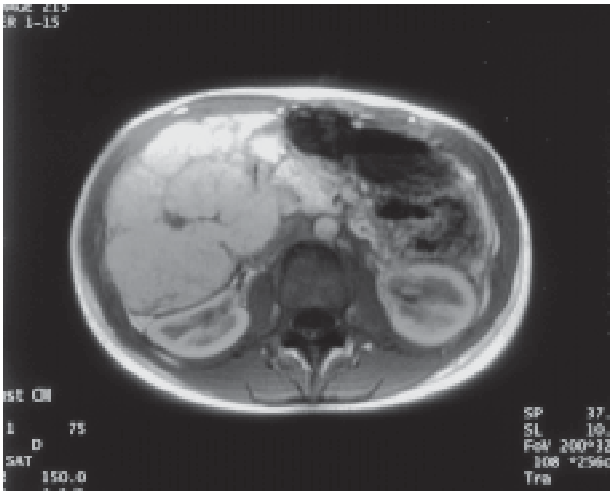

Fig. 5c. Breath-hold in phase postcontrast image of focal nodular hyperplasia with a central scar.

able by US or CT, and can differentiate FNH from metastasis[13,14,16,17]. FNH appears on MRI as an isointense or slightly hypointense lesion on T1 weighted images (Fig. 5a). On T2 weighted images, FNH is isointense with liver parenchyma with a scar of high signal intensity (Fig. 5b). The central scar appears hypointense on T1 weighted images and hyperintense on T2 weighted images due to fresh connective tissue with rich vascularity.

In the early phase, FNH shows strong enhancement of the parenchymal part of the lesion compared to normal liver parenchyma, while the central scar remains unenhanced[18-21] (Fig. 5c). In the delayed phase, the parenchymal part of the lesion becomes isointense with the liver, while the central scar shows increase in signal intensity. This biphasic enhancement pattern is specific for FNH. On T2 weighted images, the parenchymal part of the lesion is isointense with the liver, while the central scar exhibits high signal intensity. Hepatocellular adenoma may have slightly hypointense (Fig. 6a) or increased signal intensity on T1 weighted images due to the high glycogen content. Hemorrhage within adenoma shows high signal intensity on T1 as well as on T2 weighted images. The hypervascular nature of hepatocellular adenoma shows early enhancement after administration of contrast

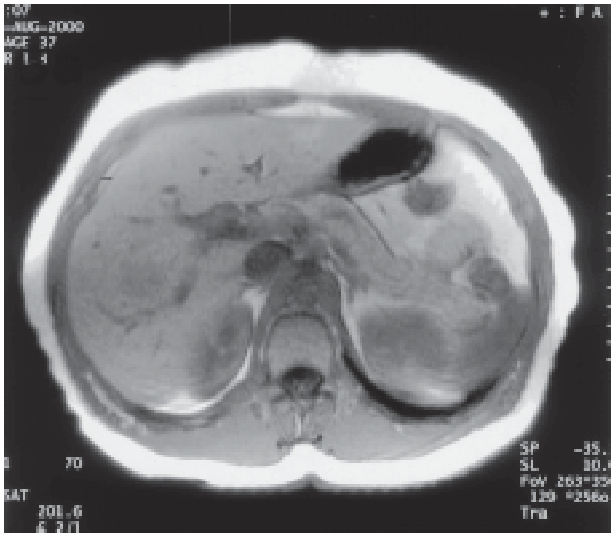

Fig. 6a Breath-hold in phase sequence showing hypointense lesion of hepatic adenoma.

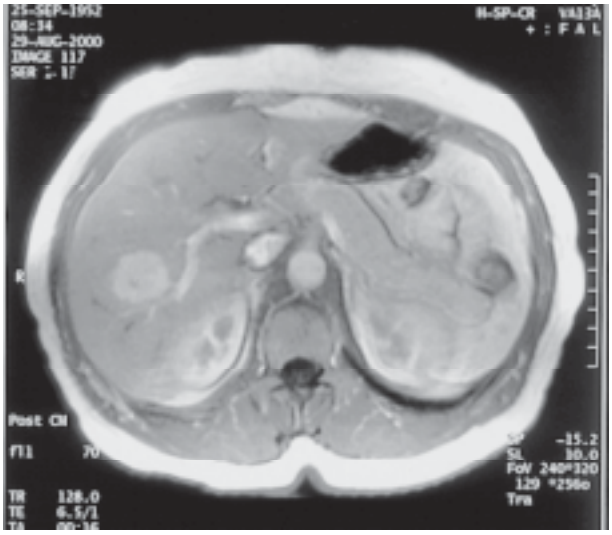

Fig. 6b. Breath-hold in phase postcontrast arterial phase image showing a early high signal intensity enhancement of the adenoma.

Fig. 6c. Breath-hold in phase delayed postcontrast image shows isointensity of the lesion with liver parenchyma.

media with rapid washout (Fig. 6b). Delayed postcontrast image demonstrates isointensity of the lesion with liver parenchyma (Fig. 6c).

Hepatocellular Carcinoma

US and CT are equally accurate in the detection of hepatocellular carcinoma[22-24]. Ultrasound appearance of hepatocellular carcinoma is variable. Small lesions are usually hypoechoic. Larger lesions have increased echogenicity. Intraluminal vessel tumor invasion is readily recognized by US. Diffuse form of hepatocellular carcinoma is very difficult to demonstrate with CT despite the application of contrast media.

MRI usually differentiates hepatocellular carcinomas from other liver lesions due to the presence of tumor capsule, intratumoral septa, daughter nodules, central scarring and tumor thrombi in portal or hepatic veins[25-29]. Hepatocellular carcinoma is predominantly supplied by the hepatic artery, which results in early arterial contrast enhancement. On T1 weighted images, hepatocellular carcinoma shows various signal intensities, from hypo- to iso- or hyperintense values[31-35] (Fig. 7a). On T2 weighted images, most of them (80%) show high signal intensity compared with liver parenchyma (Fig. 7b). Well differentiated tumors exhibit high signal intensity on T1 weighted images and isointensity on T2 weighted images. Poorly differentiated hepatocellular carcinoma demonstrates low signal intensity on T1 weighted images and hyperintensity on T2 weighted images[36]. Poorly differentiated tumors demonstrate infiltrative characteristics, whereas well differentiated tumors show only expansive pattern. Enhancement of hepatocellular carcinoma on postcontrast images depends on the degree of differentiation[37,38]. Generally, there is a peak of enhancement in the early arterial phase, whereas some of well differentiated tumors show the lack of peak enhancement during the early arterial phase (Fig. 7c). Detection of tumor capsule with MRI is important for differential diagnosis, as it has been seldom found in metastases or cholangiocarcinoma and very often in hepa-

Fig. 7a Breath-hold in phase sagittal image showing a well demarcated hypointense hepatocellular carcinoma.

Fig. 7b Breath-hold in phase postcontrast arterial phase image showing inhomogeneous enhancement of hepatocellular carcinoma with a low intensity capsule.

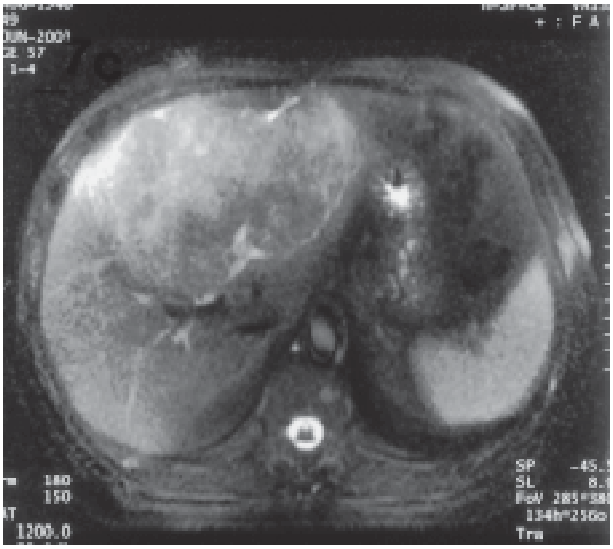

Fig. 7c Breath-hold HASTE sequence showing an inhomogeneous lesion of high signal intensity.

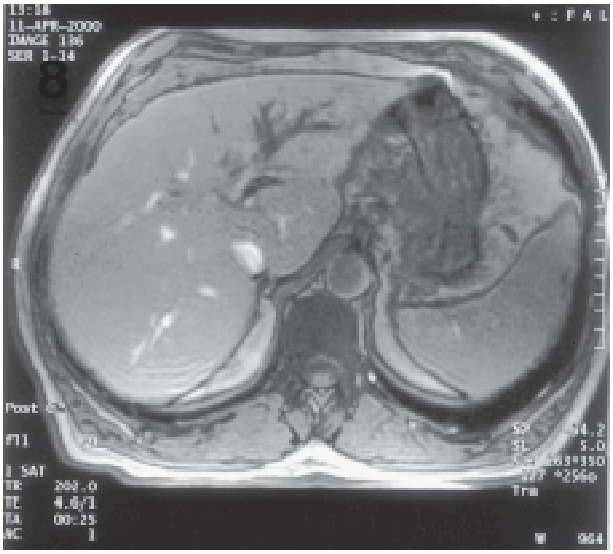

Fig. 8. Breath-hold out of phase postcontrast image with rim enhancement of cholangiocarcinoma and dilated bile ducts.

tocellular carcinoma. The capsule has low-signal intensity on T1 weighted images (Fig. 7c). Intravascular spread of hepatocellular carcinoma is an important staging and prognostic sign. MRI is capable of differentiating tumor thrombus from other thrombotic masses by demonstrating the increase of signal intensity of the thrombus on arterial postcontrast scans. Enhancement is identical to enhancement of the main tumor[39-41]. Detection and differentiation of hepatocellular carcinoma from other liver tumors is improved with hepatobiliary contrast media[42]. MRI breath-hold sequences have shown similar sensitivity and specificity as spiral CT in the detection and characterization of hepatocellular carcinoma as well as in differentiation from macroregenerative nodules[42,43]. Meticulous search for liver metastases is needed because they are frequently associated with hepatocellular carcinoma and their finding is of major importance for therapy planning.

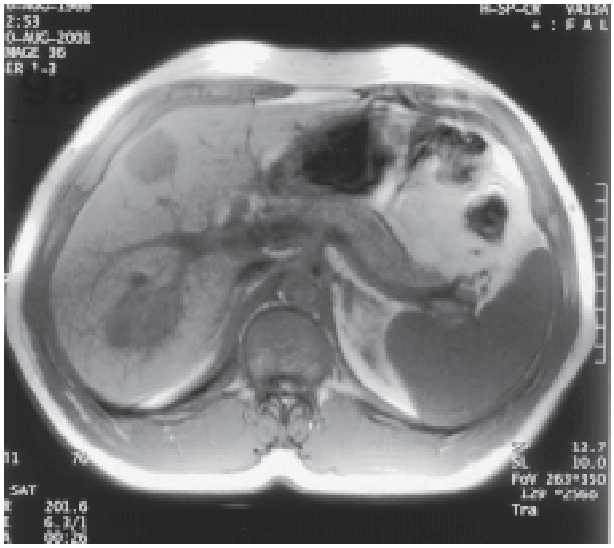

Fig. 9a Breath-hold in phase sequence with low signal intensity liver metastases of colon carcinoma.

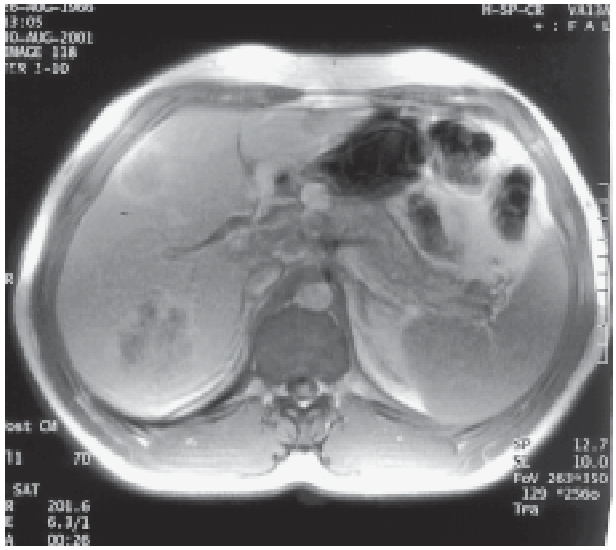

Fig. 9b Breath-hold in phase postcontrast image with rim enhancement of the lesions.

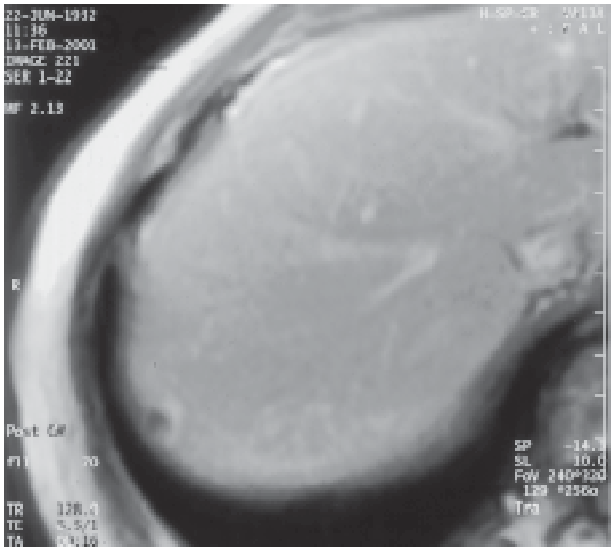

Fig. 9c Breath-hold in phase postcontrast image with rim enhancement of a 6mm metastatic lesion.

Cholangiocellular Carcinoma

Cholangiocarcinoma or peripheral cholangiocarcinoma is the second most common primary liver neoplasm after hepatocellular carcinoma. On T1 weighted images cholangiocarcinoma is mostly hypointense, and on T2 weighted images it may be of isotense or hyperintense signal intensity. On T2 weighted images, a central scar due to fibrous tissue is often present. The lesion has lobulated margins and absence of capsule. On postcontrast scans with GD-DTPA, there is slight rim enhancement (Fig. 8), less than in hemangiomas, with moderate progresive fill-in[44]. Dilatation of the peripheral bile ducts is seen in 20%-68% of cases (Fig. 8).

Metastases

Patients with liver metastases who undergo surgical resection of the secondary deposits have improved long-term survival rates compared to similar patients who do not undergo resection[45-47]. Preoperative diagnostic imaging evaluation of metastases should be performed to detect the number, size, segmental location and relationship to hepatic vasculature. Recent advances in CT, US and MRI have improved detection of liver neoplasms. CT is the established method for detection and evaluation of secondary liver deposits[23-25,48]. According to recent studies, MRI has become an important diagnostic technique for detection of focal liver lesions[49-53]. Liver tumor nodules are detected at small size and in most cases the lesions can be characterized with high reliabillity[54-60]. In spite of the newer imaging methods available, US is a sensitive and accurate modality for the identification, localization and characterization of focal hepatic abnormalities[61-64]. Because of the absence of irradiation exposure, easy use and low cost, US plays a major role in hepatic imaging.

Patients with malignant disease considered for hepatic resection should have accurate preoperative imaging evaluation, because the number and distribution of lesions de-

termines therapeutic approach. Clinical studies have shown improved survival rates after resection of primary and metastasis lesions[65-66]. There is only a few studies dealing with the sensitivity and specificity of low-field MRI compared with CT[41].

On breath-hold T1 weighted sequences, metastases demonstrate low signal intensity with rim enhancement on postcontrast studies (Fig. 9a, b, c). Metastases show signal hyperintensity compared to liver parenchyma on T2 weighted images on MRI. Most metastases have regular borders and homogeneous signal intensity, as shown by Brown *et al.* One study demonstrated the ability and advantages of detection of liver metastasis disease with low-field MR imaging *versus* contrast enhanced CT[43]. The result is comparable to conclusions of three comparative studies, stating that an intermediate field strength MR imaging is superior to contrast enhanced CT in the detection of hepatic metastases[67-68]. In contrast, some authors claim that contrast enhanced CT is superior in the detection of hepatic metastases because of better resolution and lower susceptibility to artifacts[69].

The study performed on low-field magnet has shown that T1 weighted sequence detected 51% and CT 63% of the liver lesions demonstrated by T2 weighted sequence[47]. T2 weighted images on spin-echo sequence have shown identical sensitivity in the detection of liver metastases as inversion recovery technique. CT demonstrated 92% of the lesions detected by inversion recovery technique.

Diffuse Liver Disease

Hepatomegaly is present when a length of 15.5 cm is found in the midclavicular line[69]. Values under 13 cm are within the normal range. Values between 13 and 15.5 cm are indeterminate[70].

Fatty infiltration of the liver is present in various pathologic conditions such as obesity, alcohol abuse, cirrhosis, diabetes mellitus, trauma, toxic substances, metabolic disease and others[71]. Fatty infiltration of the liver produces increased ultrasonic echogencity. CT is a method which accurately detects fatty liver infiltration with liver densities under 40 Hounsfield units. Spin-echo MRI using usual imaging techniques is not capable to detect fatty liver[72]. With the introduction of breath-hold in phase and out-of-phase sequences MRI is capable of demonstrating fatty liver deposit. There is a loss of signal on the out-of-phase sequence compared to in-phase sequence (Fig. 10a, b).

Hemochromatosis is readily demonstrated by CT and MRI. On CT, hemochromatosis appears as a diffuse increase in densities up to 95 Hounsfield units. MR spin-echo T1 weighted image shows extremely low signal intensity of liver parenchyma in hemochromatosis (Fig. 11).

Liver Cirrhosis

US, CT and MRI have no single specific echosonographic, CT density or MRI signal alteration in liver cir-

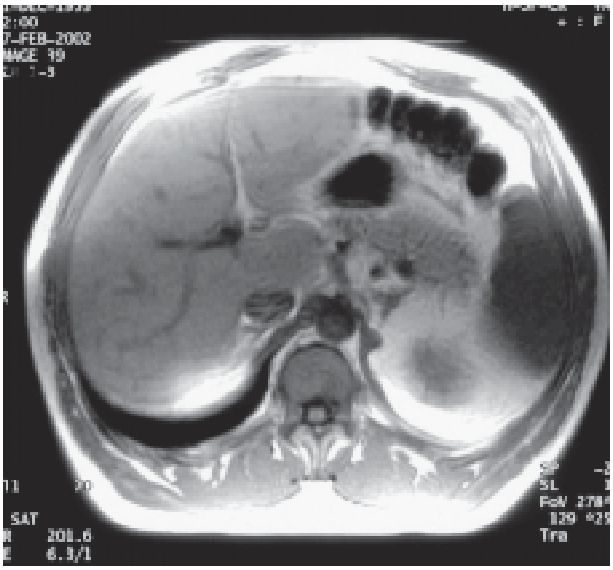

Fig. 10a Breath-hold in phase sequence showing uniform normal signal intensity of the liver.

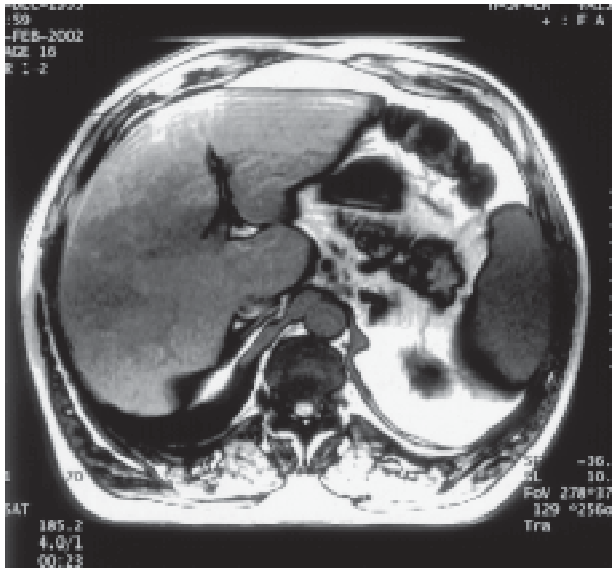

Fig. 10b Breath-thold out of phase image showing an area of lower signal intensity due to fatty liver deposit.

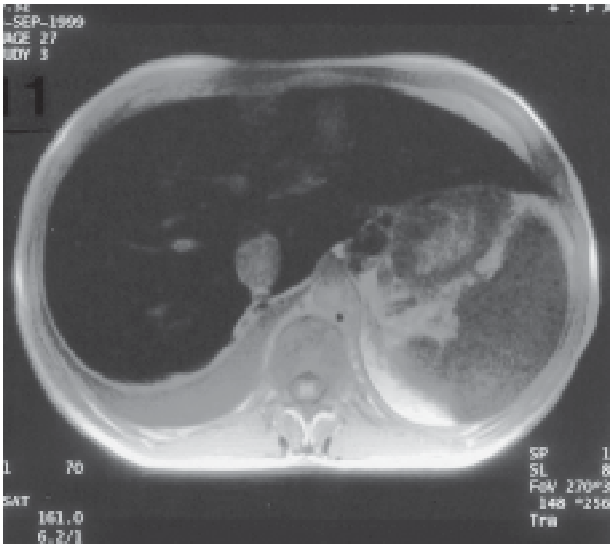

Fig. 11. Breath-hold in phase sequence showing extremely diffuse homogeneous low signal intensity of the liver due to hemochromatosis.

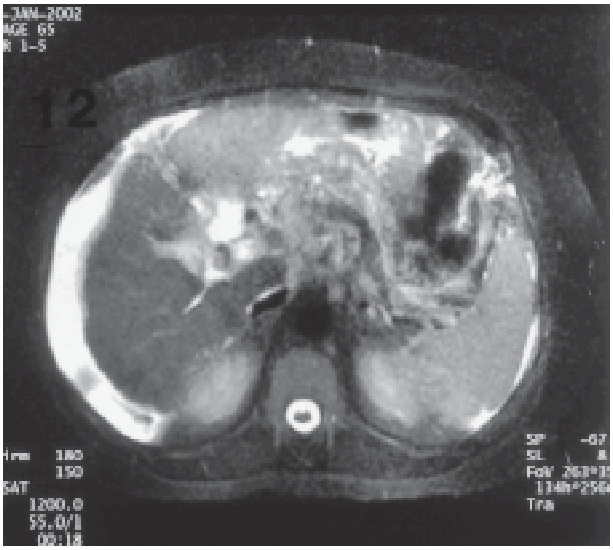

Fig. 12. Breath-hold HASTE sequence showing nodular liver surface and ascites in a cirrhotic patient.

rhosis. US echogencity, CT densities and MR signal intensities are mostly heterogeneous. The diagnosis is achieved according to specific morphologic liver changes and ascites (Fig. 12).

References

1. RUMMENY EJ, MARCHAL G. Liver imaging: clinical applications and future perspectives. Acta Radiol 1997;8:626-30.
2. MAROTTI M, HRICAK H, FRITZCHE P, CROOKS LE, HEDGCOCK MW, TANAGHO EA. Complex and simple renal cysts: comparative evaluation with MR imaging. Radiology 1987;162:679-84.
3. KARHUNEN PJ. Benign hepatic tumors and tumor like conditions in men. J Clin Pathol 1986;39:180-8.
4. ISHAK K. Benign tumors of the liver. Med Clin North Am 1975;59:995-1013.
5. MIRK P, RUBARTELLI L, BAZZOCCHI M, *et al.* Ultrasonographic patterns in hepatic hemangiomas. J Clin Ultrasound 1982;10:373.
6. SOLBIATI L, LIVRAGHY T, L De PRA L, at al. Fine needle biopsy of hepatic hemangioma with sonographic guidance. AJR Am J Roentgenol 1985;144-471.
7. LOMBARDO DV, BAKER ME, SPRITZER CE, *et al.* Hepatic hemangiomas *versus* metastases: MR differentiation at 1.5T. AJR Am J Roentgenol 1990;155:55-9.
8. EGGLLIN K, RUMMENY E, STARK DD., *et al.* Hepatic tumors: quantitative tissue characterization with MR imaging. Radiology 1990;176:107-10.
9. VAN BEERS BE, GALLEZ B, PRINGOT J. Contrast-enhanced MR imaging of the liver. Radiology 1997;203:297-306.
10. SIEWERT B, MULLER MF, FOLEY M, WIELOPOLSKI PA, FINN JP. Fast MR imaging of the liver: quantitative comparison of techniques. Radiology 1994;193:37-42.
11. REINING JW. Breath-hold fast spin echo MR imaging of the liver: a technique for high quality T2-weighted images. Radiology 1995;194:303-4.
12. ROGERS JV, MACK LA, FREENY PC, *et al.* Hepatic focal nodular hyperplasia: angiography, CT, sonography, and scintigraphy. AJR Am J Roentgenol 1981;137:983.
13. BUTCH RJ, STARK DD, MALT RA. MR imaging of hepatic focal nodular hyperplasia. J Comput Assist Tomogr 1986;10:874.
14. MATTISON GR, GLAZER GM, QUINT LE, *et al.* MR imaging of hepatic focal nodular hyperplasia: characterization and distinction from primary malignant hepatic tumors. AJR Am J Roentgenol 1987;148:711.
15. KOPP AF, LANIADO M, DAMMANN F, *et al.* MR imaging of the liver with Resovist: safety, efficacy, and pharmacodynamic properties. Radiology 1997;204: 749-56.
16. SHAMSI K, DE SCHEPPER A, DEGRYSE H, DECKERS F. Focal nodular hyperplasia of the liver: radiological findings. Abdom Imaging 1993;18:32-8.
17. BUETOW PC, PANTONGRAG-BROWN L, BUCK JL, *et al.* Focal nodular hyperplasia of the liver: radiologic-pathologic correlation. Radiographics 1996;16:369-88.
18. LEE M, HAMM B, SAINI S. Focal nodular hyperplasia of the liver: MR findings in 35 proved cases. AJR Am J Roentgenol 1991;156: 317-20.
19. MAHFOUZ AE, HAMM B, TAUPIZ M, *et al.* Hypervascular liver lesions: differentiation of focal nodular hyperplasia from ma-

lignant tumors with dynamic gadolinium-enhanced MR imaging. Radiology 1993;186:133-8.

20. MORTELE KJ, PREAT M, VAN VLIERBERGHE H, KUNNEN M, ROS PR. CT and MR imaging findings in focal nodular hyperplasia of the liver: radiologic-pathologic correlation. AJR Am J Roentgenol 2000;175:687-92.
21. GRANDIN C, VAN BEERS BE, ROBERT A, *et al.* Benign hepatocellular tumors: MRI after superparamagnetic iron oxide administration. J Comput Assist Tomogr 1995;19:412-8.
22. MILLER DL, SIMMONS JT, CHANG R, *et al.* Hepatic metastases detection: comparison of three CT contrast enhancement methods. Radiology 1987;165:785-90.
23. MOSS AA, DEAN BP, AXEL L, *et al.* Dynamic CT of hepatic masses with intravenous and intraarterial contrast material. AJR Am J Roentgenol 1982;138:847-52.
24. FOLEY WD, BERLAND LL, LAWSON TL, *et al.* Contrast enhancement technique for dynamic hepatic computed tomographic scanning. Radiology 1983;147:797-803.
25. MATSUI O, KADOYA M, SUZUKI M, *et al.* Dynamic sequential computed tomography during arterial portography in detection of hepatic neoplasms. Radiology 1983;146:721-7.
26. BLAKEBOROUGH A, WARD J, WILSON D, *et al.* Hepatic lesion detection at MR imaging: a comparative study with four sequences. Radiology 1997;203:759-65.
27. HARISINGHANI M, SAINI S, WIESSLEDER R, *et al.* Differentiation of liver hemangiomas and hepatocellular carcinomas at MR imaging enhanced with blood-pool contrast agent code-7227. Radiology 1997;202:687-91.
28. REIMER P, RUMMENY EJ, DALDRUP HE, *et al.* Enhancement characteristics of liver metastases, hepatocellular carcinomas, and hemangiomas with Gd-EOB-DTPA: preliminary results with dynamic MR imaging. Eur Radiol 1997;7:275-80.
29. WHITNEY WS, HERFKENS RJ, JEFFREY RB, *et al.* Dynamic breath-hold multiplanar soiled gradient-recalled MR imaging with gadolinium enhancement for differentiating hepatic hemangiomas from malignancies at 1,5 T. Radiology 1993;189: 863-70.
30. HAMMERSTINGL R, VOGL TJ, SCHWARTZ W. Contrast-enhanced MRI of focal liver lesions: differentiation and detection of primary and secondary liver lesions using Resovist-enhanced *versus* gadolinium-enhanced MRI in the same patient. Acta Radiol 1998:5:75-9.
31. KANEMATSU M, HOSHI H, MURAKAMI T, *et al.* Detection of hepatocellular carcinoma in patients with cirrhosis: MR imaging *versus* angiographically assisted helical CT. AJR Am J Roentgenol 1997;169:1507-15.
32. LABERGE JM, LAING FC, LE MP, *et al.* Hepatocellular carcinoma: assessment of resectability by computed tomography and ultrasound. Radiology 1984;152:485.
33. SHEU JC, CHEN DS, SUNG JL, *et al.* Hepatocellular carcinoma: US evolution in the early stage. Radiology 1985;155:463.
34. SUBRAMANYAM BR, BALTHAZAR EJ, HILTON, *et al.* Hepatocellular carcinoma with venous inavasion. Radiology 1984;150:793.
35. HUGHES KS, ROSENSTEIN RB, SONGHORABODI S, *et al.* Resection of the liver for colorectal carcinoma metastases a multi-institutional study of long-term survivors. Dis Colon Rectum 1988;31:1-4.
36. GLAZER GM, AISEN AM, FRANCIS IR, GROSS BH, GYVES JW, ENSMINGER WD. Evaluation of focal hepatic masses: a comparative study of MRI and CT. Gastrointest Radiol 1986;11:263-8.
37. WEYMAN PJ, LEE JKT, HEIKEN JP, *et al.* Prospective evaluation of hepatic metastases: CT scanning, CT angiography, and MR imaging. Radiology 1986;138:623-7.
38. STARK DD, WITTENBERG J, EDELMAN RR, *et al.* Detection of hepatic metastases: analysis of pulse sequence performance in MR imaging. Radiology 1986;159:365-70.
39. HONDA H, KANEKO K, MAEDA T, *et al.* Small hepatocellular carcinoma on magnetic resonance imaging. Relation of signal intensity to angiographic and clinicopathologic findings. Invest Radiol 1997;32 161-8.
40. IMAEDA T, KANEMATSU M, MOCHIZUKI R, GOTO S, SAJI S, SHIMOKAWA K. Extracapsular invasion of small hepatocellular carcinoma: MR and CT findings. J Comput Assist Tomogr 1994;18: 755-60.
41. MURAMATSU Y, NAWANO S, TAKAYASU K, *et al.* Early hepatocellular carcinoma: MR imaging. Radiology 1991;181:209-13.
42. DACHMAN AH, ROS PR, GOODMAN ZD, *et al.* Nodular regenerative hyperplasia of the liver: clinical and radiologic observations. AJR Am J Roentgenol 1987; 148:717-22.
43. SIEGELMAN ES, OUTWATER EK, FURTH EE, *et al.* MR imaging of hepatic nodular regenerative hyperplasia. J Magn Reson Imaging 1995;5:730-2.
44. VILGRAIN V, VAN BEERS B, FLEJOU JF, *et al.* Intrahepatic cholangiocarcinoma: MRI and pathologic correlation in 14 patients. J Comput Assist Tomogr 1997; 21:59-65.
45. HEIKEN JP, WEYMAN PJ, LEE JKT, BALFE DM, PICUS D, BRUNT EM, WAYNE FLYE M. Detection of focal hepatic masses: prospective evaluation with CT, deleyed CT, CT during arterial portography, and MR imaging. Radiology 1989;171:47-51.
46. ADSON MA, VON HEERDEN JA, ADSON MH, WAGNER JS, ILSTRUP DM. Resection of hepatic metastases from colorectal cancer. Arch Surg 1984;119:647-51.
47. MAROTTI M, SUČIĆ Z, KLARIĆ R, KROLO I, BABIĆ N, GORANIĆ T, ŠUNIĆ M. Magnetic resonance imaging and computerized tomography in detection of liver metastases. Croat J Gastroenterol Hepatol 1993;2:19-23.
48. BERNARDINO ME, ERWIN BC, STEINBERG HV, *et al.* Delayed hepatic CT scaning: increased confidence and improved detection of hepatic metastases. Radiology 1986;159:71-4.
49. BYDDER GM, STEINER RE, BLUMGARTH LH, KHENIA S, YOUNG IR. MR imaging of the liver using short T1 inversion recovery sequences. J Comput Assist Tomogr 1985;9:1084-9.
50. PALING MR, ABBITT PL, MUGLER JP, BROKEMAN JRI. Liver metastases: optimization of MR imaging pulse sequence at 1T. Radiology 1988;167:695-9.
51. DOUSSET M, WEISSLEDER R, HENDRICK RE, STARK DD, FRETZ CJ, ELIZONDO G, HAHN PF, SAINI S, FERRUCCI JT. Short T1 inversion recovery imaging of the liver: pulse sequence optimization and comparison with spin echo imaging. Radiology 1989;171:327-3.
52. SCHUMAN WP, BARON RL, PETERS MJ, TAZIOLI PK. Comparison of STIR and spin echo MR imaging at 1.5 T in 90 lesions of the chest, liver, and pelvis. AJR Am J Roentgenol 1989;152:853-9.
53. BUTCH RJ, STARK DD, MALT RA. MR imaging of hepatic focal nodular hyperplasia. J Comput Assist Tomogr 1986;10:874-7.
54. VOGL TJ, HAMMERSTINGL R, SCHWARTZ W. Superparamagnetic iron oxide-enhanced *versus* gadolinium-enhanced MR imaging for differential diagnosis of focal liver lesions. Radiology 1996;198:881-7.

55. VOGL TJ, HAMMERSTINGL R, SCHWARTZ W. Magnetic resonance imaging of focal liver lesions. Comparison of the superparamagnetic iron oxide Resovist *versus* gadolinium-DTPA in the same patient. Invest Radiol 1996;31:696-708.
56. RUMMENY EJ, TORRES CG, KURDZIEL JC, NILSEN G, OP DE BEECK B, LUNDBY B. MnDPDP for MR imaging of the liver: results of an independent image evaluation of the European phase III studies. Acta Radiol 197;38:638-42.
57. CAUDANA R, MORANA G, PIROVANO GP, *et al.* Focal malignant hepatic lesions: MR imaging enhanced with gadolinium benzyloxypropionictetra-acetate (Gd-BOPTA). Preliminary results of phase II clinical application. Radiology 1996;199:513-20.
58. OUDKERK M, HEUVEL AG, WIELOPOLSKI P, *et al.* Hepatic lesions: detection with ferumoxide-enhanced T1-weighted MR imaging. Radiology 1997; 203: 449-56.
59. SHAMSI K, BALZER T, SAINI S, *et al.* Superparamagnetic iron oxide particles (SHU 555 A): evaluation of efficacy in three doses for hepatic MR imaging. Radiology 1998;206:365-71.
60. LENCIONI R, DONATI F, CIONI D, PAOLICCI A, CICORELLI A, BARTOLOZZI C. Detection of colorectal liver metastases: prospective comparison of unenhanced and ferumoxide-enhanced magnetic resonance imaging at 1.5 T, dual-phase spiral CT, and spiral CT during arterial portography. MAGMA 1998;7:76-87.
61. FEDERLE MP, FILLY RA, MOSS AA. Cystic hepatic neoplasms: complementary roles of CT and sonography. AJR Am J Roentgenol 1981;136:345.
62. SEXTON CC, ZEMAN RA. Correlation of computed tomography, sonography and gross anatomy of the liver. AJR Am J Roentgenol 1983;141:711.
63. MARKS WM, FILLY RA, CALLEN PW. Ultrasonic anatomy of the liver: a review with new applications. J Clin Ultrasound Med 1979;7:137.
64. HOLM J, JACOBSEN B. Accuracy of dynamic ultrasonography in the diagnosis of malignant liver lesions. J Clin Ultrasound Med 1986;5:1.
65. CADY B, MCDEROTT WV. Major hepatic resection for metachronous metastases from colon cancer. Ann Surg 1985;201:204-9.
66. Registry of Hepatic Metastases: Resection of the liver for colorectal carcinoma metastases – a multi-institutional study of indications for resection. Surgery 1988;103:278-88.
67. REINING JW, DWYER AJ, MILLER DL, *et al.* Liver metastases detection comparative sensitivities of MR imaging and CT scanning. Radiology 1987;162:43-7.
68. STARK DD, WITTENBERG J, BUTCH RJ, FERRUCCI JT. Hepatic metastases: randomized, controlled comparison of detection with MR imaging and CT. Radiology 1987;165:399-406.
69. WERNECKE K, RUMMENY E, BONGARTZ G, *et al.* Detection of hepatic masses in patients with carcinoma: comparative sensitivities of sonography, CT and MR imaging. Am J Roentgenol 1991;157:731-9.
70. GOSINK BB, LAYMASTER CE. Ultrasonic determination of hepatomegaly. JCU 1981;9:37.
71. SCATARIGE JC, SCOTT WW, DONOVAN PJ, *et al.* Fatty infiltration of the liver: ultrasonographic and computed tomographic correlation. J Ultrasound Med 1984;3:9.
72. STARK DD, GOLDBERG HI, MOSS AA, BASS NM. Chronic liver disease: evaluation by magnetic resonance. Radiology 1984;150:149-51.
73. STARK DD, MOSELEY ME, BACON BR, *et al.* Magnetic resonance imaging and spectroscopy of hepatic iron overload. Radiology 1985;154:137-42.